Journal of
Synchrotron Radiation

ISSN 0909-0495

Received 11 June 2012
Accepted 4 September 2012

A variable ultra-short-pathlength solution cell for XAFS transmission spectroscopy of light elements

John L. Fulton,[a]* Mahalingam Balasubramanian,[b] Van-Thai Pham[a] and George S. Deverman[c]

[a]Chemical and Materials Sciences Division, Pacific Northwest National Laboratory, Richland, WA 99354, USA, [b]X-ray Science Division, Argonne National Laboratory, Argonne, IL 60439, USA, and [c]Energy Processes and Materials Division, Pacific Northwest National Laboratory, Richland, WA 99354, USA. E-mail: john.fulton@pnnl.gov

An X-ray absorption fine-structure spectroscopy (XAFS) cell that is suitable for solution-phase studies of the light elements in the series from Na^+ and Ca^{2+} is described. This cell has an ultra-short pathlength that can be remotely adjusted using a miniature stepper-motor drive and thereby readily provides transmission pathlengths in the range from submicrometer to several hundred micrometers. The flexibility to vary the pathlength enables acquisition of high-quality XAFS spectra and also allows one to check for potential distortions in the spectra from thickness effects. The primary components are mostly commercially available optical parts. The performance of this device is demonstrated at the Cl *K*-edge (2.8 keV) for several different aqueous Cl^- solutions.

Keywords: X-ray absorption fine structure; XAFS; low-*Z* cell; short pathlength.

1. Introduction

The light elements in the third-row and early fourth-row series (including Na, Mg, Al, Si, P, S, Cl, K and Ca) contain six of the most prevalent elements in the earth's crust. In their various chemical states they play central roles in a wide variety of geochemical and biochemical processes. Some of these elements (*e.g.* P and S) also play important roles in catalysis and energy storage. The chemical state of these elements can be probed using the method of X-ray absorption fine structure (XAFS). XAFS provides detailed molecular structure information on the coordination state including bond distances, bond disorder, coordination symmetry, oxidation state and the chemical identities of coordination species and even in disordered systems. In earlier studies of these light elements, XAFS spectroscopy has been used to determine the hydration structure about aqueous ions (Dang *et al.*, 2006) (Cl^-, K^+ and Ca^{2+}) both under ambient conditions and for temperatures up to approximately 700 K in water (Fulton *et al.*, 2004, 2006). More recently the contact ion pair structure between Cl^- and hydronium (H_3O^+) has been elucidated (Fulton & Balasubramanian, 2010). Further, XAFS studies have provided important information on protonation of aqueous phosphate species (Rouff *et al.*, 2009) and for ion chemical states in rechargeable lithium/sulfur batteries (Gao *et al.*, 2011). However, many of these studies were limited by the difficulty of preparing samples with suitably short pathlengths. In this report we describe an adjustable short-pathlength XAFS transmission cell that is specifically designed to address liquid-phase solutions for this series of light elements. The *K*-edge absorption energies for these elements span the range from 1 keV to 4.5 keV. This energy range also coincides with the *L*-edge energies for the series of elements above Zn including almost all of the second-row transition metals up to Cd that are of primary interest for catalysis. This energy range also covers the $M_{4,5}$-edges for the lanthanides and actinides. Thus this ultra-short-pathlength cell is also useful for *L*-edge studies of the second-row transition metals and *M*-edge studies of the actinides and lanthanides.

The cell is optimized for transmission measurements of solutes at moderate to high concentrations. In this case transmission measurements provide superior signal-to-noise ratios since the fluorescence yields of the light elements are rather low. However, the challenge is that the X-ray absorbance lengths at these low energies (1 keV to 4.5 keV) are rather short and therefore both the windows and the sample pathlengths need to be short. In order to maximize the transmission of the X-ray beam through the sample, the use of thin membrane windows (100–500 nm thick) having relatively little beam attenuation is preferred. Thin Si_3N_4 membrane windows were first used by Yang for an XAFS transmission study of water (Yang & Kirz, 1987). Recently, Wernet *et al.* (Schreck *et al.*, 2011) and Nagasaka *et al.* (2010) have reported a significant improvement on the concept for very low energies (300–1000 eV) including the study of the O *K*-edge of liquid water. Huthwelker *et al.* (2010) developed a cell for O *K*-edge

studies of individual aerosol particles under controlled atmospheres. Variants of these cells have been described for both transmission (Näslund *et al.*, 2005) and fluorescence measurements (Aziz, 2010; Aziz *et al.*, 2006; Guo & Luo, 2010; Edwards & Myneni, 2006; Freiwald *et al.*, 2004). In this report we describe a cell that is optimized for both X-ray absorption near-edge spectroscopy (XANES) and extended X-ray absorption fine-structure spectroscopy (EXAFS) at somewhat higher energies. This cell is optimal for those elements having edge energies in the range from 1 keV to 4.5 keV. These require relatively longer pathlengths when compared with cells used for soft X-rays (<1 keV). This cell also uses membrane windows; however, one of the windows is connected to a stepper-motor drive. Using this approach a broad range of pathlengths (1–500 µm) can be selected by remotely adjusting the stepper-motor position. The resolution of the stepper-motor drive is 50 nm, thereby allowing achievement of pathlengths well below 1 µm. In this design the parts having wetted surfaces are machined from a chemically resistant polymeric material whereas the primary mechanical components are mostly commercially available. This allows for more ready implementation of the method at a multitude of beamlines.

Finally, the cell is suitable for transmission measurements for a variety of different aqueous, organic, ionic liquid and nanoparticle-containing phases. Although designed specifically for transmission measurement there are instances where the device could be potentially beneficial for fluorescence measurements at 45°, since the adjustable pathlength feature of the device would allow for optimizing the effective sample thickness to minimize self-absorption effects from concentrated samples.

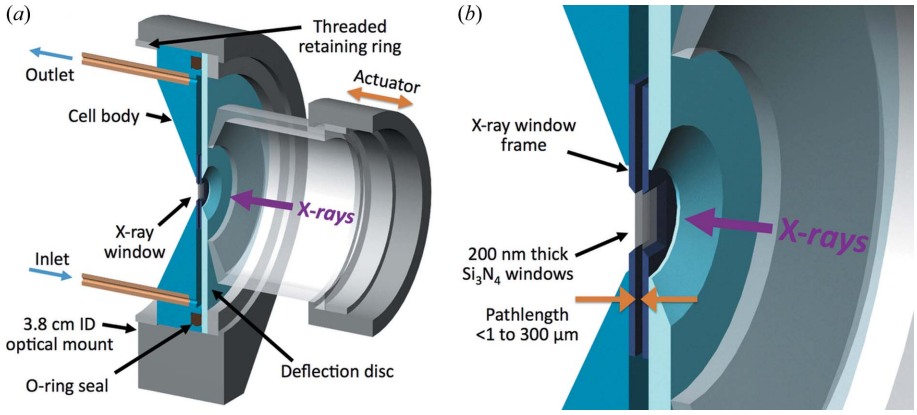

Figure 1
(*a*) Cross section of the X-ray transmission cell. (*b*) An expanded view of the X-ray window region.

2. Cell design

Schematics of the primary components of the cell are shown in Fig. 1. Images of the entire cell are shown in Fig. 2. The sample liquid is contained between two polyether ether ketone (PEEK) discs. PEEK provides very high chemical resistance for a broad range of compounds. One of the 3.8 cm-diameter discs is essentially rigid and contains the connections for introducing the sample through 1.6 mm outer-diameter PEEK tubing (Upchurch Scientific) into the cell. The other disc is flat, thin and flexible and is machined to a relatively high thickness uniformity (±0.025 mm). These two discs are sealed together using an elastomeric O-ring to create the disc-shaped liquid-filled cavity between the two PEEK plates. The thin PEEK disc is deflected by applying a uniform circular load near the center of the disc in the region where the X-ray beam passes through the cell. The load is applied using a miniature stepper-motor translation stage (Micos, VT-21 S) having 50 nm resolution. In this way the X-ray pathlength through the liquid can be remotely adjusted in the range from approximately 1 to 500 µm. The deflection of this plate under load can be calculated using an analytical formula for a flat circular plate having a constant thickness, with the outer edge fixed, and with a line load on the inner circumference (Roark & Young, 1982). Fig. 3 shows typical deflections for a 3.8 cm-diameter PEEK disc of various thicknesses.

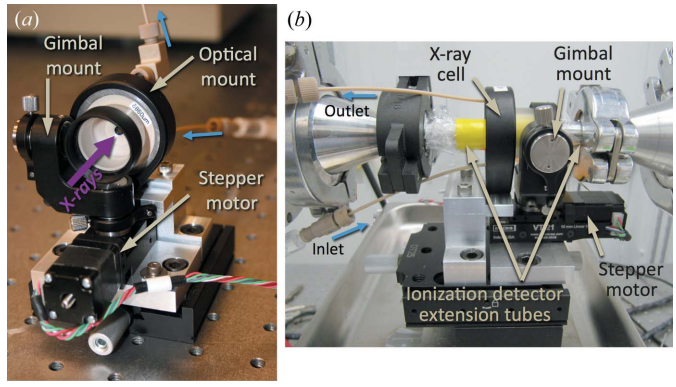

Figure 2
(*a*) Image of the assembled transmission cell. (*b*) View of the transmission cell installed between two gas-ionization detectors.

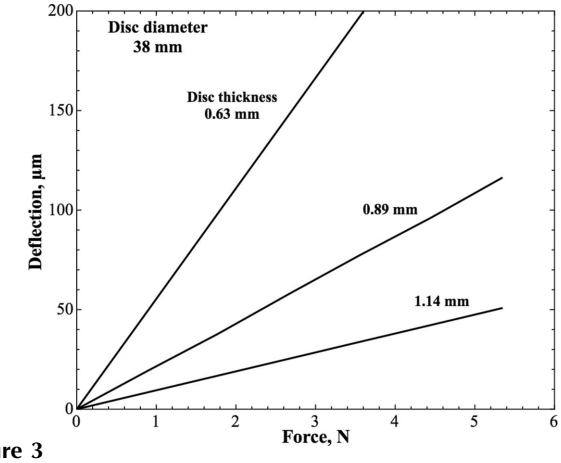

Figure 3
Plot showing the amount of deflection of the sample cell disc (PEEK) as a function of the force by the actuator. The choice of different disc thicknesses can be used to cover different deflection ranges for a given actuator force.

Portions of the device use standard optical components routinely found at synchrotron beamlines. The two PEEK discs are held together using a standard lens mount (Thorlabs, LMR1.5). The actuator shown in Fig. 1(*a*) is driven by the stepper-motor drive (Micos, VT-21 S). To be sure that the actuator applies the load uniformly, it is attached to a gimbal (Thorlabs, #GMB1) that is mounted directly onto the miniature stepper-motor drive. The gimbal mount assures that the circular load is evenly distributed and that the load remains perpendicular to the surface of the deflection disc. The X-ray windows are two silicon nitride (Si_3N_4) windows (Norcada) that are affixed to the inner surfaces of the PEEK discs. These 2 mm × 2 mm by 200 nm-thick Si_3N_4 membranes are part of a larger 7.5 mm × 7.5 mm by 500 µm-thick Si frame (Norcada). These frames are then attached to the PEEK discs using a silicone-resin-based high-vacuum adhesive (Vacseal, SPI Supplies). The two 200 nm-thick Si_3N_4 membranes provide >75% transmission in the range from 1 to 4.5 keV. The maximum pressure differential across these membrane windows is approximately 1 bar. Before filling the sample cell with liquid, the stepper motor is fully retracted to open the gap between the Si_3N_4 windows. This allows the solute solution to fully replenish the region between the windows. The gap is then reduced for the XAFS measurement. The maximum velocity of the translator is limited to allow the fluid between the windows to be expelled, without build up of pressure, as the gap is being reduced. The configuration shown in Fig. 2 is intended for use under ambient temperatures although the thicker of the two sample containment discs ('cell body' in Fig. 1) could be constructed from a metal alloy and thereby electrically heated to provide temperature control up to approximately 373 K.

Even though the Si_3N_4 windows are quite thin they can introduce artifacts from the Si edge (1839 eV) and the Si XAFS structure (from the Si_3N_4) into the sample spectra in this energy region. An alternate window material for this spectral region is 800 nm-thick CVD diamond membranes that are also provided mounted on Si frames (Applied Diamond). Two 800 nm-thick CVD diamond membranes provide >70% transmission in the region above 1.5 keV and provide a clean background in this region.

As shown in Figs. 2(*b*) and 4, the solution is introduced into the cell using a syringe. A second, open-top, vessel is used as a receiver to capture excess fluid during the filling process. For the ultra-thin X-ray windows used in this study, a small amount of hydrostatic pressure is sufficient to cause a small distension of the Si_3N_4 membrane windows. For this reason the elevation of the meniscus in the receiver vessel should approximately coincide with the elevation of the X-ray window. Small changes in the elevation of the receiver can be used to fine-tune the gap between the two X-ray windows. The receiver could also be attached to a vertical translator and stepper motor to remotely fine-tune the gap.

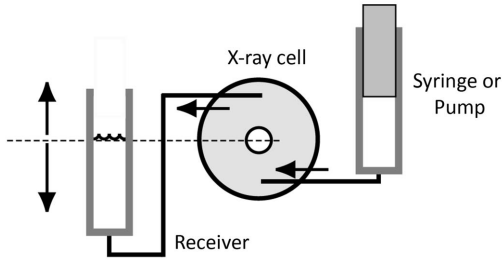

Figure 4
Schematic of the liquid filling system. The elevation of the meniscus in the receiver controls the hydrostatic pressure at the elevation of the X-ray windows.

3. XAFS results

Fig. 5 shows a series of Cl *K*-edge XAFS spectra of hydrated Cl^- in aqueous 6 *M* NaCl. Fig. 6 shows the XANES spectra for a series of polyoxoanions of chlorine. All of these chlorine *K*-edge (2822 eV) XAFS spectra were acquired at the bending-magnet beamline at the Advanced Photon Source, Argonne National Laboratory (XSD/PNC, Sector 20). A single 10 min scan is sufficient to obtain high-quality transmission spectra at this beamline. The incident beam was focused to a small spot (650 µm × 350 µm) using an Al_2O_3/Pt-coated toroidal

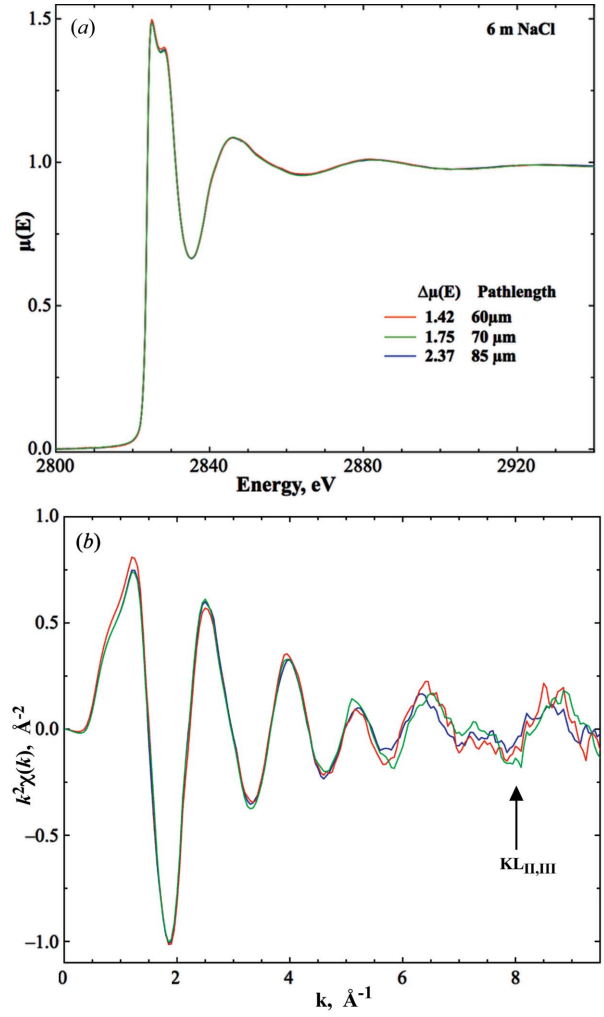

Figure 5
(*a*) Cl *K*-edge, normalized $\mu(E)$ and (*b*) k^2-weighted XAFS plots for a single 10 min scan.

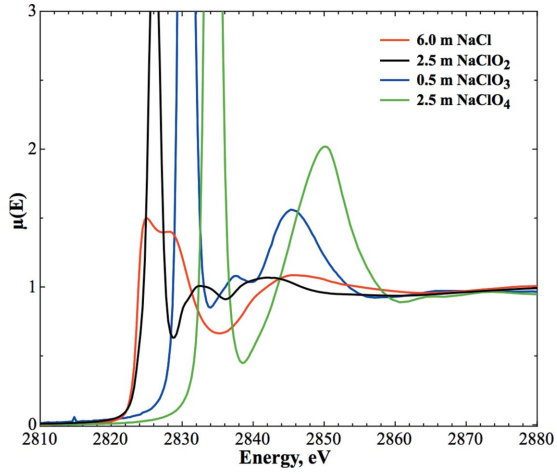

Figure 6
Normalized XANES $\mu(E)$ plots for Cl^- and various ClO_x^- species for a single scan (10 min).

mirror. The Al_2O_3 coating suppresses the influence of the Pt *M*-edges (Heald, 2011). Harmonic contamination was minimized by setting a Ni-coated X-ray mirror to ∼10.5 mrad, inserted in front of the beam-defining slits near the I_0 detector. In combination with ∼25% crystal detuning, a high degree of harmonic rejection is attained. Energy calibration was accomplished using the first inflection point of the Ar *K*-edge (3205.9 eV). The estimated incident flux was $\sim 1 \times 10^{10}$ photon s^{-1}.

We used two standard gas-ionization detectors for transmission measurements at the Cl *K*-edge. The 18 cm-long upstream ionization detector, I_0, was filled with a 4% N_2/96% He mixture whereas the 30 cm-long downstream detector, I_T, was filled with a 35% N_2/65% He mixture. As shown in Fig. 2(*b*), the ends of these two detectors were extended to within 1–2 mm of the Si_3N_4 cell windows so that the air gap was reduced to minimize beam absorption by air. Each of these extenders was terminated with 4 µm-thick Prolene films. All of the beam path (*e.g.* slits and harmonic rejection mirror) upstream from these detectors was helium purged. As an alternate configuration the entire cell assembly could be placed inside a helium-purged tank or enclosure that is a common component of many low-energy beamlines.

In Fig. 5, three different sets of $\mu(E)$ spectra for a 6 *M* NaCl solution are presented. The spectra were acquired using three different pathlength settings, 60, 70 and 85 µm, resulting in absorption-edge heights of 1.42, 1.75 and 2.37, respectively. In the case of the 85 µm pathlength the beam transmission through the solution is only about 5%. The fact that the three spectra are almost identical, especially in the strongly absorbing white-line region about 2825 eV, indicates that the windows are parallel as required to prevent any leakage effects (Heald, 1988). The resulting $k^2\chi(k)$ plots are shown in Fig. 5(*b*) after background subtraction. Notably, the spectra are almost identical, again supporting the equivalency of the different pathlengths and the parallelism of the windows. The Cl—O bond for the hydrated $Cl^-{\cdot}H_2O_n$ is quite disordered (Fulton & Balasubramanian, 2010) with a Debye–Waller factor of approximately 0.024 $Å^2$. This means that the primary oscillations from the Cl—H_2O scattering are strongly damped at higher *k*. Even so, with a single 10 min scan, the signal-to-noise ratio is sufficiently high to capture five or six oscillations from the backscattering of water. There is a well known multielectron excitation ($KL_{II,III}$) at $k = 8$ $Å^{-1}$ that interferes with the XAFS oscillation at higher *k* (Fulton & Balasubramanian, 2010). Finally, Fig. 6 shows the XANES region for aqueous Cl^- and three different polyoxyanions of chlorine. The obtained spectra show the expected sensitivity to Cl speciation and validate the ability to obtain distortion-free spectra with high signal-to-noise ratios. The cell is easily loaded for each sample and the optimization of the pathlength while the cell is in the beam provides for efficient evaluation of multiple samples of this type.

This work was supported by the US Department of Energy's (DOE) Office of Basic Energy Sciences, Division of Chemical Sciences, Geosciences and Biosciences. PNNL is operated for the Department of Energy by Battelle. XSD/PNC facilities at the Advanced Photon Source, and research at these facilities, are supported by the US Department of Energy, Basic Energy Sciences, a major facilities access grant from NSERC, the University of Washington, Simon Fraser University, the Pacific Northwest National Laboratory and the Advanced Photon Source. Use of the Advanced Photon Source is also supported by the US Department of Energy, Office of Science, Office of Basic Energy Sciences, under Contract DE-AC02-06CH11357.

References

Aziz, E. F. (2010). *J. Electron Spectrosc. Relat. Phenom.* **177**, 168–180.
Aziz, E. F., Zimina, A., Freiwald, M., Eisebitt, S. & Eberhardt, W. (2006). *J. Chem. Phys.* **124**, 114502.
Dang, L. X., Schenter, G. K., Glezakou, V. A. & Fulton, J. L. (2006). *J. Phys. Chem. B*, **110**, 23644–23654.
Edwards, D. C. & Myneni, S. C. (2006). *J. Phys. Chem. A*, **110**, 11809–11818.
Freiwald, M., Cramm, S., Eberhardt, W. & Eisebitt, S. (2004). *J. Electron Spectrosc. Relat. Phenom.* **137**, 413–416.
Fulton, J. L. & Balasubramanian, M. (2010). *J. Am. Chem. Soc.* **132**, 12597–12604.
Fulton, J. L., Chen, Y., Heald, S. M. & Balasubramanian, M. (2004). *Rev. Sci. Instrum.* **75**, 5228–5231.
Fulton, J. L., Chen, Y., Heald, S. M. & Balasubramanian, M. (2006). *J. Chem. Phys.* **125**, 094507.
Gao, J., Lowe, M. A., Kiya, Y. & Abruna, H. D. (2011). *J. Phys. Chem. C*, **115**, 25132–25137.
Guo, J. H. & Luo, Y. (2010). *J. Electron Spectrosc. Relat. Phenom.* **177**, 181–191.
Heald, S. M. (1988). *X-ray Absorption: Principles, Applications, Techniques of EXAFS, SEXAFS and XANES*, edited by D. C. Koningsberger and R. Prins, pp. 87–118. New York: John Wiley and Son.
Heald, S. M. (2011). *Nucl. Instrum. Methods Phys. Res. A*, **649**, 128–130.
Huthwelker, T., Zelenay, V., Birrer, M., Krepelova, A., Raabe, J., Tzvetkov, G., Vernooij, M. G. & Ammann, M. (2010). *Rev. Sci. Instrum.* **81**, 113706.
Nagasaka, M., Hatsui, T., Horigome, T., Hamamura, Y. & Kosugi, N. (2010). *J. Electron Spectrosc. Relat. Phenom.* **177**, 130–134.

Näslund, L. A., Lüning, J., Ufuktepe, Y., Ogasawara, H., Wernet, P., Bergmann, U., Pettersson, L. G. & Nilsson, A. (2005). *J. Phys. Chem. B*, **109**, 13835–13839.
Roark, R. J. & Young, W. C. (1982). *Formulas for Stress and Strain.* New York: McGraw-Hill.
Rouff, A. A., Rabe, S., Nachtegaal, M. & Vogel, F. (2009). *J. Phys. Chem. A*, **113**, 6895–6903.
Schreck, S., Gavrila, G., Weniger, C. & Wernet, P. (2011). *Rev. Sci. Instrum.* **82**, 103101.
Yang, B. X. & Kirz, J. (1987). *Phys. Rev. B*, **36**, 1361–1364.